

VACUUM REQUIREMENTS FOR HEAVY ION RECIRCULATING INDUCTION ACCELERATORS†

J. J. BARNARD and S. S. YU

Lawrence Livermore National Laboratory, Livermore, CA 94550, USA

and

A. FALTENS

Lawrence Berkeley Laboratory, Berkeley, CA 94720.

(Received 3 December 1990)

We examine the requirements of the vacuum system for the LLNL/LBL recirculating induction accelerator concept. We reexamine processes, including beam stripping, background gas ionization, intra-beam charge exchange and desorption of gas molecules from the wall due to the incident ionized gas molecules and stripped ions, in the context of the proposed recirculator. We discuss implications for the vacuum system layout and estimate the cost of such a system.

1 INTRODUCTION

In a recirculating heavy ion induction accelerator, the residence time of an ion beam in the accelerator can be a factor of ten or more longer than in a linear accelerator, due to the lower average accelerating gradient in the recirculator. The allowed background gas density in the recirculator is required to be lower by a factor roughly equal to the ratio of the residence times. In addition, the beam will desorb gas molecules from the wall, and will propagate, on subsequent laps around the recirculator, through the beam-induced desorbed gas, placing more stringent requirements on the vacuum pumping rates. A number of processes have been identified in previous work (cf. Refs. 1-4) that cause loss of the heavy ion beam; we shall rely heavily on this work. As in previous work, a number of uncertainties exist in our knowledge of cross sections and desorption coefficients. The main purpose of this paper is to make our best estimate of how severe the vacuum and pumping requirements might be in a heavy ion recirculator used as the driver for an inertial confinement fusion power plant. In particular, we will focus on the recirculator design presented by Yu *et al.* at this conference.

† Work performed under the auspices of the U.S. Department of Energy by LLNL under contract W-7405-ENG-48, and at LBL by the Director, Office of Energy Research, Advanced Energy Projects Division, U.S. D.O.E. under contract DE-AC03-76SF00098.

2 PROCESSES

For the purpose of this paper, we consider four processes, which have been identified in Ref. 3 as contributing to possible losses of the heavy ion beam: Stripping, Background Gas Ionization, Beam Induced Gas Desorption, and Beam-Beam Charge Exchange. We briefly review these processes.

2.1 Stripping

Stripping occurs when an electron is stripped off of a heavy ion, upon an interaction with a gas particle:



Here HI represents heavy ion and G stands for gas molecule. In the recirculator, due to the presence of the bending magnets, a particle of a charge state that is higher or lower by one electron charge will be lost in a distance that is short compared to the ring radius. The cross-section for stripping and excitation in the Born approximation σ_{sB} is calculated in Ref. (5) and graphed in Ref. (4), and is given approximately by:

$$\sigma_s < \sigma_{sB} \cong \begin{cases} 1.0 \times 10^{-17} (Z_b/92) \beta^{-2} \text{ cm}^2 & (\text{N}_2) \\ 1.0 \times 10^{-18} (Z_b/92) \beta^{-2} \text{ cm}^2 & (\text{H}_2) \end{cases} \quad (1)$$

Here N_2 and H_2 are the background gases, Z_b is the atomic number of the heavy ion beam, and σ_s is the stripping cross section alone. This cross-section is valid for large ion velocities ($v_i \gg \alpha c$, where α is the fine structure constant and c is the speed of light). At low energies, the cross section increases with increasing energy. At intermediate energies a broad peak in the cross section occurs.

Where the exact turn-over occurs is uncertain. Low energy experimental data (Refs. 6 and 7) indicates that for uranium ions ($Z_b = 92$) being stripped by N_2 background gas at energies around 1–2 MeV, the cross section already appears quite flat and is around $1.0 \times 10^{-15} \text{ cm}^2$.

2.2 Gas Ionization

Here a beam particle ionizes a background gas particle:



The Born cross section for excitation and ionization σ_{ionB} is calculated in Ref. (5), which in the limit of large β we summarize roughly as:

$$\sigma_{ion} < \sigma_{ionB} \cong 1.0 \times 10^{-16} (Z_b/92)^{1.2} \beta^{-2} \text{ cm}^2. \quad (2)$$

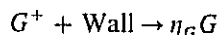
Here σ_{ion} is the actual ionization cross section. Again, low energy data for lighter ions suggests that, upon scaling to heavier ions, the maximum may be as low as $\sim 10^{-15} \text{ cm}^2$ for beam particles of atomic mass $A_b \cong 200$ on molecular nitrogen gas (cf, e.g., Ref. 8). This number should be regarded as quite uncertain, however.

As pointed out in Ref. (3), gas ionization does not lead to beam loss directly, but

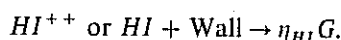
rather indirectly through interactions with the walls, which causes increased gas density.

2.3 Beam Induced Gas Desorption

Here the ionized gas particles, in the presence of the strong radial electric field of the heavy ion beam are driven to the wall with energies up to tens of keV. There they desorb η_G gas molecules per incident gas ion. Stripped or neutralized heavy ions may also contribute η_{HI} gas molecules per incident heavy ion. Symbolically,



and



The energy gain E_{ion} of the ions due to the space charge of the beam is approximately

$$(2I/\beta_i c) \ln[b/a] = 18 \text{ keV } (I/180\text{A})(0.3/\beta)(\ln[b/a]/0.7),$$

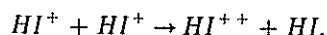
where I is the beam current, $\beta_i c = v_i$ is the ion beam velocity, b is the pipe radius and a is the average beam radius. At these energies sputtering coefficients η_G are, according to Refs. (9) and (10), experimentally measured to be on the order of a few ($\cong 5$). These sputtering coefficients are found from specially treated clean surfaces. The actual surfaces found in a recirculator may be "dirtier," but may in fact be cleaned by the process of beam desorption. Large uncertainty exists in our knowledge of η_G and η_{HI} . In Ref. (10) an empirical formula for sputtering coefficients as a function of energy, ion and target species is given, with coefficients determined from experimental data, so that an extrapolation to high energy may be attempted. For lead ions ($A = 207$) impinging upon iron targets ($A = 56$) with energies of 1 to 10 GeV, impinging normally upon the surface, the desorption coefficient is calculated to be ~ 0.05 to 0.002 respectively, decreasing inversely with energy. As the energy increases, the ions penetrate deeper within the metal surface and therefore desorb fewer surface atoms. (In Ref. 19 it is shown that η_{HI} could be many orders of magnitude larger than this estimate, however.) Also, as pointed out in Ref. 11, the ions will not have normal incidence. In a recirculator, neutralized or stripped ions will have glancing incidence and can dislodge many surface particles, increasing the effective η_{HI} for heavy ions by several orders of magnitude.

A possible solution is to ensure that the stripped or neutralized heavy ions strike surfaces at normal incidence by placing circular apertures or scrapers periodically within the beam pipe. Minimum grazing angles θ of the heavy ions impinging upon the surface are of the order $(\Delta r/R)^{1/2}$, where Δr is the clearance distance between beam and pipe, and R is the recirculator radius. In order to intercept the misguided ions, scrapers would need to have an aspect ratio (radial extent $\Delta r_{\text{scraper}}$ divided by the distance between scrapers $L_{\text{scraper}} \geq \theta$). So $L_{\text{scraper}} \leq \Delta r_{\text{scraper}}(R/\Delta r)^{1/2}$. For the large ring of Ref. 12, $R \cong 400$ m and $\Delta r \cong 3$ cm, the maximum spacing would be about 3.5 m, (for $\Delta r_{\text{scraper}} = \Delta r$). Much smaller $\Delta r_{\text{scraper}}$ is possible (to avoid intercepting the beam) with correspondingly smaller L_{scraper} .

We note that η_G and η_{HI} are based on sputtering coefficients of beams for clean metallic surfaces. In an accelerator, desorption of wall molecules will depend on the state of the condensed gases that are on and within the pipe surface. The effect of the beam may be to clean the surface, reducing desorption rates but probably not reducing them below the sputtering rates described above. Further, the sputtered materials will include metallic atoms which will have different resorption properties than the desorbed gas atoms. Thus the vacuum properties may vary during an initial "conditioning" time in which condensed gases are removed, and may change over longer time scales as "micro-roughening" of the surface occurs. All of these subjects are areas of future research activities, and need to be resolved before a recirculator is constructed. For the purpose of this paper, however, we lump all of these processes into time-independent desorption coefficients based on sputtering coefficients.

2.4 Beam-Beam Charge Exchange

In this process two singly charged heavy ions interact transferring one electron, resulting in a doubly charged ion and a neutral ion:



Experimental data exists for singly charged bismuth ($Z_b = 83$, $A_b = 209$) in the energy range of interest (Refs. 13 and 14). We parameterize their cross-section measurements approximately as:

$$\sigma_{ce} \cong \begin{cases} 2.1 \times 10^{-16} (E_{cm}/10 \text{ keV})^{0.62} \text{ cm}^2 & \text{if } E_{cm} < 19 \text{ keV} \\ 1.8 \times 10^{-16} (E_{cm}/10 \text{ keV})^{0.94} \text{ cm}^2 & \text{if } E_{cm} > 19 \text{ keV} \end{cases} \quad (3)$$

Here E_{cm} is the energy in the heavy ion's center-of-mass frame. Note that σ_{ce} also includes beam ionization, $HI^+ + HI^+ \rightarrow HI^{++} + HI^+ + e^-$, which contributes (to a lesser extent) to beam loss as well.

3 BACKGROUND GAS EVOLUTION

The fluid equations may be used to understand the evolution of the gas density within the accelerator pipe. We follow a similar line of reasoning that is pursued in the study of proton storage rings, such as the Intersecting Storage Ring (ISR) at CERN (e.g., Refs. 15-17).

The continuity equation (assuming variation only in z and t) becomes:

$$\frac{\partial}{\partial t} n_g + \frac{\partial}{\partial z} n_g v_z = \mu \sigma_s v_i n_b n_g - \frac{S_{lin}}{A_p} n_g + q_{eff}. \quad (4)$$

Here,

$$\mu = \left[\frac{\sigma_{ion}}{\sigma_s} \eta_G + \eta_{HI} \right] \left[\frac{V_{beam}}{V_{pipe}} \right], \quad (5)$$

n_g is the background gas number density, n_b is the heavy ion beam number density, v_b is the heavy ion velocity, v_z is the z component of background gas fluid velocity at time t and position along acceleration direction z ; S_{lin} is the linear pump strength (dimensions unit volume per unit time per unit distance), A_p is the cross-sectional area of pipe = πb^2 , where b = pipe radius; and $q_{eff} = q + q_{ce}$ is the sum of the intrinsic outgassing rate per unit distance along the accelerator q and the outgassing rate due to desorbed gases from heavy-ions which have been lost due to charge exchange q_{ce} . Note that $q = 2Q_0/b$, where Q_0 is the intrinsic outgassing rate per unit surface area and b is the pipe radius; $q_{ce} = \eta_{HI} n_b^2 \sigma_{ce} v_{cm} (V_{beam}/V_{pipe})$; V_{beam} is the total volume of the beam = $\pi a^2 v_p t_p$, where a = beam radius, t_p = pulse duration; V_{pipe} = volume of the pipe = $\pi b^2 C$ where C is the circumference of the recirculator; v_{cm} is the average thermal velocity of the ions in the co-moving ion frame.

In Eq. (4) the left-hand side represents the normal conservation of particles. In addition, on the right-hand side there are sources (the first and third terms) and sinks (the second term). The second term represents the effect of distributed (linear) pumps. The first term arises from the desorption of wall molecules by stripped beam particles and ionized background gas particles, while the third term represents intrinsic outgassing plus desorption of wall molecules from beam-beam charge exchange.

The momentum equation (again assuming variation only in z and t) is:

$$\frac{\partial}{\partial t} n_g v_z + \frac{\partial}{\partial z} n_g v_z^2 = - \frac{v_z n_g}{\tau} - \frac{kT}{m_g} \frac{\partial n_g}{\partial z} \tag{6}$$

Here, τ is the mean time between wall collisions, k is Boltzmann's constant, T is the gas temperature, and m_g is the mean mass of the gas molecules.

The second term is the ram pressure term of the background gas and is ignorable, and the first term is the inertial term. The time t_s for sound traveling at the sound speed c_s to cross the distance between vacuum pumps L is usually much less than the residence time Δt in the recirculator. Since some fraction of Δt is the time scale over which density changes are of interest, we also ignore the first term in the momentum equation. The third term represents the effects of the collisions of gas particles with the walls of the pipe, i.e., the conductance of the pipe, and for timescales of interest, this term is balanced by the pressure gradient (cf. Ref. 18):

$$n_g v_z \cong - \frac{\tau kT}{m_g} \frac{\partial n_g}{\partial z} \tag{7}$$

Using Eq. (7) to eliminate v_z , the continuity equation becomes:

$$\frac{\partial n_g}{\partial t} = \mu \sigma_s v_i n_b n_g - \frac{S_{lin}}{A_p} n_g + q_{eff} + \frac{\tau kT}{m_g} \frac{\partial^2 n_g}{\partial z^2} \tag{8}$$

The boundary conditions at the lumped pump locations at $z = \pm L/2$ require that gas flow into the pump aperture is matched by the gas being pumped out: (cf. Ref. [16]):

$$S_{lump} n_g |_{z=L/2} = 2 n_g v_z A_p |_{z=L/2} = \frac{2 \tau k T A_p}{m_g} \frac{\partial n_g}{\partial z} \Big|_{z=L/2} \tag{9}$$

Here L is the distance between lumped pumps, and S_{lump} is the lumped pumping speed (with dimensions of unit volume per unit time).

Averaging over the distance between pumps, L , yields an equation for the z -averaged gas density \bar{n} :

$$\frac{d\bar{n}}{dt} = \mu\sigma_s v_i n_b \bar{n} - \frac{S_{\text{lin}}}{A_p} \bar{n} + q - \frac{S_{\text{lump}}}{A_p L} n_g|_{z=L/2} + q_{\text{eff}}. \quad (10)$$

Now the gas density at a vacuum pump is some fraction f of the average gas density: $n_g|_{z=L/2} = f\bar{n}$ where

$$f \cong \begin{cases} 1 - \frac{t_{\text{diff}}}{4t_{\text{pump}}} & \text{if } t_{\text{diff}} \ll t_{\text{pump}} \\ \frac{\pi^2 t_{\text{pump}}}{4 t_{\text{diff}}} & \text{if } t_{\text{diff}} \gg t_{\text{pump}} \end{cases}. \quad (11)$$

Here $t_{\text{pump}} = LA_p/S_{\text{lump}}$ and is a lumped pumping time; $t_{\text{diff}} = 3L^2/(v_i^2\tau)$ and is the diffusion time of a gas particle through the pipe due to wall collisions; and $\tau = 2b/v_i$ and is the time between wall collisions. The factor f was obtained by assuming a $\cos([\pi - \varepsilon]z/L)$ density dependence in the strong pumping limit and a $\cos(2\varepsilon z/L)$ in the weak pumping limit and then solving for the small quantity ε . The variable f should be correct to within a factor of order unity. Physically, if the pumps are sufficiently close together, or the pump strengths are sufficiently weak, there will be a small density gradient, and the pumps will act as if they are distributed uniformly along the pipe. We may define an effective total linear pump speed $S_T = S_{\text{lin}} + fS_{\text{lump}}/L$ and an effective net pumping time $t_{\text{net}} = A_p/(\mu n_b \sigma_s v_i A_p - S_T)$ for which the average gas density equation becomes:

$$\frac{d\bar{n}}{dt} = q_{\text{eff}} + \frac{\bar{n}}{t_{\text{net}}}. \quad (12)$$

Note that t_{net} is positive (and is thus an exponential growth time) if the gas desorption rate outpaces the pumping rate.

4 BEAM EVOLUTION EQUATION

As discussed in section 2, stripping and charge exchange lead to losses from the beam:

$$\frac{dn_b}{dt} = -\sigma_s v_i n_b \bar{n} - \sigma_{ce} v_{cm} n_b^2. \quad (13)$$

We assume that the fractional beam loss is small (even though this may lead to large changes in background gas density). Let $n_b(t) = n_{b0} - \delta n_b$. Define $x = \delta n_b/n_{b0}$, then Eq. (13) becomes:

$$\frac{dx}{dt} \cong \sigma_s v_i \bar{n} + \sigma_{ce} v_{cm} n_{b0}. \quad (14)$$

5 APPROXIMATE SOLUTIONS TO THE COUPLED BEAM/GAS EQUATIONS

In addition to assuming that the fractional beam losses are small ($x \ll 1$), we tentatively make a number of simplifying assumptions to facilitate solution of the coupled equations, (12) and (14). In assumption 1, we assume that the quantities $\sigma_s v_i$, $\sigma_{\text{ion}} v_i$, $\sigma_{\text{ce}} v_{\text{cm}}$, η_{HI} , and η_G are constants equal to their average values during the transit of each of the four rings. In assumption 2, we make plausible assumptions about the ionization and stripping cross sections: $\sigma_s = \text{Min}[1.0 \times 10^{-15}, 3.0 \times 10^{-18}(Z_b/92)\beta^{-2}] \text{ cm}^2$ and $\sigma_i = \text{Min}[1.0 \times 10^{-15}, 3.0 \times 10^{-17}(Z_b/92)^{1.2}\beta^{-2}] \text{ cm}^2$. Here, the cross sections are reduced from Eqs. (2) and (3) by a factor ~ 3 to take account of the probable lower mean molecular weight of the gas and the inclusion of excitations in the Born cross sections. Using assumption (1), Eq. (12) has the solution:

$$\bar{n} = -q_{\text{eff}} t_{\text{net}} + (n_{g0} + q_{\text{eff}} t_{\text{net}}) \exp(t/t_{\text{net}}) \quad (15)$$

Here $n_{g0} = \bar{n}$ at $t = 0$. Inserting Eq. (15) into Eq. (14) yields:

$$x = (-\sigma_s v_i q_{\text{eff}} t_{\text{net}} + n_{b0} \sigma_{\text{ce}} v_{\text{cm}}) t + \sigma_s v_i t_{\text{net}} (n_{g0} + q_{\text{eff}} t_{\text{net}}) (\exp[t/t_{\text{net}}] - 1) \quad (16)$$

After the residence time in the recirculator Δt the fraction of the beam that is lost to the walls is denoted x_f . The gas density at $t = 0$ that is required to obtain a beam loss of x_f is found by solving Eq. (16) for n_{g0} :

$$n_{g0} = \frac{x_f + (\sigma_s v_i t_{\text{net}} q_{\text{eff}} - n_{b0} \sigma_{\text{ce}} v_{\text{cm}}) \Delta t}{\sigma_s v_i t_{\text{net}} (\exp[\Delta t/t_{\text{net}}] - 1)} - q_{\text{eff}} t_{\text{net}}. \quad (17)$$

If n_{g0} is greater than given by Eq. (17), the beam loss will be greater than x_f . We have found that when pumping rates are just sufficient, $t_{\text{net}} > 0$, i.e., the gas density increases exponentially during the pulse despite relatively large vacuum pumps. In that case the gas density is maximum at $t = \Delta t$ and has value $n_{g\text{max}}$ given by:

$$n_{g\text{max}} = -q_{\text{eff}} t_{\text{net}} + (n_{g0} + q_{\text{eff}} t_{\text{net}}) \exp[\Delta t/t_{\text{net}}]. \quad (18)$$

We may use the relatively large dead time between pulses $t_d (> \sim 0.1 \text{ s})$ to reduce the gas density back to n_{g0} . Defining the total pump time $t_s = A_p/S_T$, the final density at the end of the dead time n_{gf} is given by:

$$n_{gf} = q t_s + (n_{g\text{max}} - q t_s) \exp[-t_d/t_s]. \quad (19)$$

Requiring that $n_{gf} = n_{g0}$, Eqs. (18) and (19) may be used to solve for n_{g0} to give:

$$n_{g0} = \frac{q t_s - (q_{\text{eff}} t_{\text{net}} + q t_s) \exp[-t_d/t_s] + q_{\text{eff}} t_{\text{net}} \exp[\Delta t/t_{\text{net}} - t_d/t_s]}{1 - \exp[\Delta t/t_{\text{net}} - t_d/t_s]}. \quad (20)$$

In Fig. (1), we plot the required n_{g0} in Eqs. (17) and (20) as a function of the total linear pump rate S_T for parameters that characterize the large ring of Ref. 12. It is apparent that as the pump rate is increased a larger initial gas density can be tolerated linear pump rate S_T for parameters that characterize the large ring of Ref. 12. It is apparent that as the pump rate is increased a larger initial gas density can be tolerated

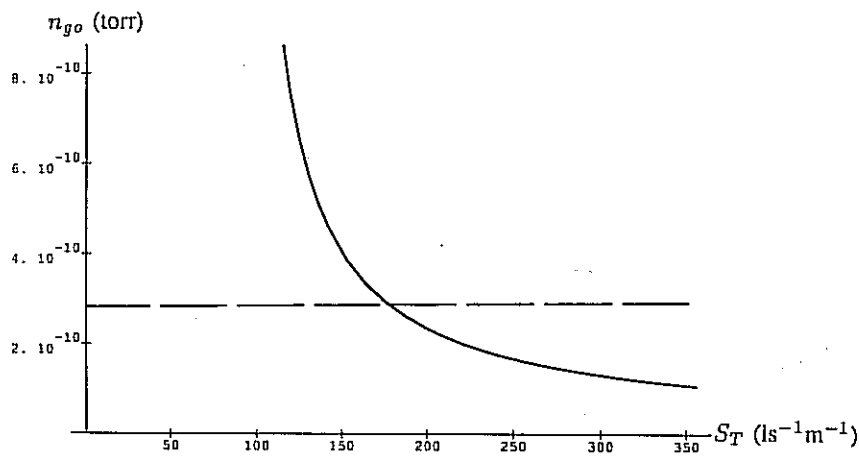


FIGURE 1 The gas density at the entrance of a beam pulse into the large ring of Ref. (12) is plotted as a function of the linear pump rate S_T . The dashed curve is the required initial density (Eq. 17) necessary to obtain a given fractional beam loss x_f . The solid curve (Eq. 20) is the initial gas density that is obtained at the given pump rate. The curves indicate that as the pump rate is increased a larger initial gas density can be tolerated to achieve a given x_f , while a lower gas density is actually achieved. The minimum pump rate required to obtain x_f occurs at the intersection of the two curves.

for a given x_f while a smaller initial gas density is actually obtained. The value of S_T at the intersection of the curves S_{crit} represents the minimum value of S_T for which the beam loss is no more than x_f . The evolution of the gas density, for a pump rate $S_T = S_{crit}$ is plotted in Figure (2), again for large ring parameters. Having obtained the effective pump rate S_T , we may set $f \cong 1$ in Eq. (11) to determine the maximum distance L_{max} such that the pumps are pumping on essentially the average density \bar{n} .

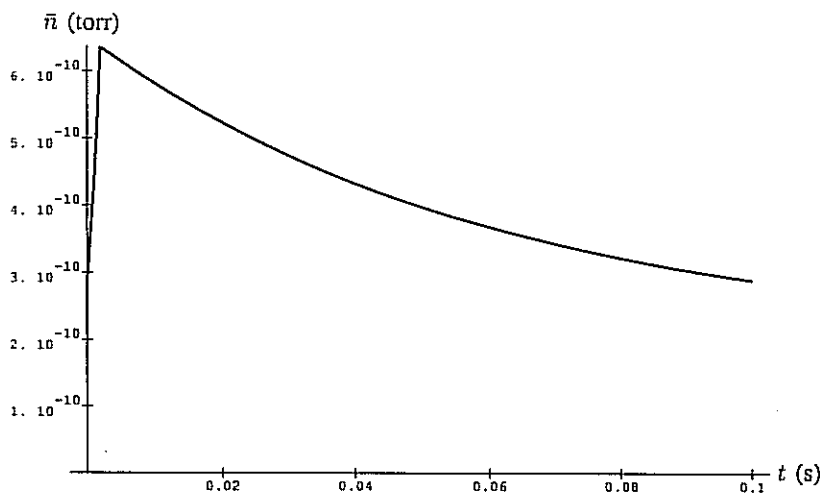


FIGURE 2 Evolution of the gas density as a function of time, at the minimum pump rate (see Fig. 1) and parameters of the large ring of Ref. (12) (see Table 1).

Allov
Char
Outg
Strip
Ioniz
Chrg
Deso
Deso
Initia
Max.
Effic
Max.
Total
 E_{em} (
Ion I
Curri
Pulse
Resic

· 1

F.
pump
para
we l
on e
ring
sma
\$9 li
requ
10⁻⁷
cost:
tech
of re
secti
of ar
so th
of th

ACK

We
and
prov

TABLE 1
Vacuum Parameters for the Recirculator Rings of Ref. 23

	IR ^a	LER ^a	MER ^a	HER ^a
Allowed Beam Loss	0.01	0.01	0.02	0.02
Charge Exchange Loss	0.0	0.0004	0.0007	0.0096
Outgassing Rate (torr 1/s cm ²)	10 ⁻¹¹	10 ⁻¹¹	10 ⁻¹¹	10 ⁻¹¹
Stripping Cross Sec. (cm ²)	1.0 10 ⁻¹⁵	1.0 10 ⁻¹⁵	5.0 10 ⁻¹⁶	5.2 10 ⁻¹⁷
Ionization Cross Sec. (cm ²)	1.0 10 ⁻¹⁵	1.0 10 ⁻¹⁵	1.0 10 ⁻¹⁵	5.5 10 ⁻¹⁶
Chrg. Exchng. Cross Sec. (cm ²)	7.1 10 ⁻¹⁸	2.2 10 ⁻¹⁷	5.4 10 ⁻¹⁷	1.3 10 ⁻¹⁶
Desorption Coeff. (Gas)	5	5	5	5
Desorption Coeff. (heavy Ion)	4	2	0.3	0.01
Initial Gas Density (torr)	8.8 10 ⁻¹¹	1.0 10 ⁻¹⁰	1.3 10 ⁻¹⁰	2.9 10 ⁻¹⁰
Max. gas Density (torr)	2.9 10 ⁻¹⁰	3.5 10 ⁻¹⁰	3.8 10 ⁻¹⁰	6.4 10 ⁻¹⁰
Effective Pump Rate (liters m)	687	529	388	178
Max. Dist. Between Pumps (m)	1.3	1.3	1.3	1.5
Total Cost of Vacuum Pumps (10 ⁶ \$)	8.3	5.4	12.8	16.5
E _{cm} (keV)	0.042	0.260	1.11	4.41
Ion Energy (average) (MeV)	10.0	54.0	479	4640
Current/Beam (Average) (A)	1.6	5.6	29	182
Pulse Duration (Average) (μs)	63	18	3.5	0.55
Residence Time Δt (ms)	5.4	2.0	2.1	1.9

^a IR, LER, MER, and HER stand for Injector-, Low-Energy-, Medium-Energy-, and High-Energy Ring, respectively.

For each of the four rings of the recirculator, we calculate some of the required pumping parameters based on the model we have described. In Table 1, we list these parameters, as well as some of the assumed parameters we have employed. Note that we have assumed a 2% loss in the high energy ring where the impact of beam loss on efficiency is greatest, whereas we tolerate a 1% loss of particles in the low energy ring and injector rings where cross sections are largest but where the rings are much smaller. We estimate the cost of such a system, by assuming a unit cost of \$9 liter⁻¹·s⁻¹, which we estimate is achievable using cryopumps. As can be seen, required initial densities (converted to initial pressures at 300 K) are ~ a few times 10⁻¹⁰ torr, effective pumping rates are in the 100's to 1000's of liter⁻¹·s⁻¹ m⁻¹ and costs are in the tens of millions of dollars. This seems to indicate that vacuum technology development and vacuum costs will not require a disproportionate share of recirculator resources. Since there are large uncertainties in our knowledge of cross sections, sputtering coefficients, and other parameters, our intent is to use this type of analysis to indicate the sensitivity on pumping rates and cost on these coefficients, so that future experimental or theoretical work can be focused on the most sensitive of these parameters.

ACKNOWLEDGEMENTS

We wish to express thanks to W. Barletta and M. Newton for useful conversations, and to H. Patton for sharing his considerable expertise on vacuum systems, and providing cost estimates and pumping scenarios.

REFERENCES

1. Y. K. Kim, in *ERDA Summer Study of Heavy Ions for Inertial Fusion*, Lawrence Berkeley Laboratory report LBL-5543, (1976) pp. 11, 58.
2. G. H. Gillespie, in *ERDA Summer Study of Heavy Ions for Inertial Fusion*, Lawrence Berkeley Laboratory report LBL-5543, (1976) 59.
3. D. Blechschmidt and H. J. Halama, in *Proceedings of the HIF Workshop* (Brookhaven National Laboratory, 1977), BNL-50769 (1977) p. 136.
4. G. H. Gillespie, in *Proceedings HIF Workshop* (Brookhaven National Laboratory, 1977), BNL-50769, (1977) p. 45.
5. G. H. Gillespie, Y.-K. Kim, and K. Cheng, *Phys. Rev. A*, **17**, (1978) 1284.
6. H. H. Lo, and W. L. Fite, *Atomic Data* **1**, (1970) 305.
7. R. C. Dehmel, H. K. Chau and H. H. Fleischmann, *Atomic Data* **5**, (1973) 231.
8. H. S. W. Massey and E. H. S. Burhop, *Electronic and Ionic Impact Phenomena*, (Clarendon, Oxford, 1952).
9. M. Kaminsky, *Atomic and Ionic Impact Phenomena on Metal Surfaces*, (Springer-Verlag, N.Y., 1965).
10. N. Matsunami, Y. Yamamura, Y. Itikawa, N. Itoh, Y. Kazumata, S. Miyagawa, K. Morita, R. Shimizu and H. Tawara, *Atomic Data and Nuclear Data Tables* **31**, (1984) 1.
11. A. Faltens, Lawrence Berkeley Laboratory technical note HIFAR Note 75 (1986).
12. S. S. Yu, J. J. Barnard, A. Friedman, L. V. Griffith, D. W. Hewett, H. C. Kirbie, V. K. Neil, M. A. S. Newton, A. C. Paul, L. L. Reginato, G. E. Russell, W. M. Sharp, J. H. Wilson, T. F. Godlove, R. O. Bangerter and D. L. Judd, these *Proceedings*.
13. F. Melchert, E. Salzborn, I. Hofman, R. W. Muller and V. P. Shevelko, *Nucl. Instrum. Meth.* **A278**, (1969) 65.
14. E. Salzborn, *Journal de Physique*, Colloque C1, Supplement au n° 1, Tome 50, (1989) C1-207.
15. C. Benvenuti, R. Calder and O. Grobner, *Vacuum* **37**, (1987) 699.
16. O. Grobner and R. S. Calder, *IEEE Trans. Nucl. Sci.* **NS-20**, (1973) 760.
17. D. Blechschmidt, *IEEE Trans. Nucl. Sci.* **NS-24**, (1977) 1379.
18. A. Roth, *Vacuum Technology*, (North-Holland, Amsterdam, 1982).
19. D. G. Koshkarev, *Part. Acc.*, (1984), 1.

f
I
b
a
c

n
te

1

A
cc
cc
fo
st
H
nc
wl
ca
wi
de
de

2

HIL
stri
ask
anc

—
†
U.S.